

# ChemComm

Accepted Manuscript



This is an *Accepted Manuscript*, which has been through the Royal Society of Chemistry peer review process and has been accepted for publication.

*Accepted Manuscripts* are published online shortly after acceptance, before technical editing, formatting and proof reading. Using this free service, authors can make their results available to the community, in citable form, before we publish the edited article. We will replace this *Accepted Manuscript* with the edited and formatted *Advance Article* as soon as it is available.

You can find more information about *Accepted Manuscripts* in the [Information for Authors](#).

Please note that technical editing may introduce minor changes to the text and/or graphics, which may alter content. The journal's standard [Terms & Conditions](#) and the [Ethical guidelines](#) still apply. In no event shall the Royal Society of Chemistry be held responsible for any errors or omissions in this *Accepted Manuscript* or any consequences arising from the use of any information it contains.

## ARTICLE

# Monolayer protected gold nanoparticles with metal-ion binding sites : Functional systems for chemosensing applications

Cite this: DOI: 10.1039/x0xx00000x

C. Pezzato, S. Maiti, J. L.-Y. Chen, A. Cazzolaro, C. Gobbo, L. J. Prins\*

Received 00th January 2012,

Accepted 00th January 2012

DOI: 10.1039/x0xx00000x

www.rsc.org/

In this review we describe the use of monolayer protected gold nanoparticles (Au NPs) for chemosensing applications. The attention is focused on a special subclass of Au NPs, namely those that contain binding sites for metal ions in the monolayer. It will be shown that these systems are very well-equipped for metal ion sensing as the complexation of the metal ions can affect the properties of the system in many ways leading towards detectable output signals even at very low analyte concentrations. In addition, the presence of metal ions in the monolayer themselves can serve as recognition units for the highly selective interaction with small organic molecules or biomacromolecules. Key examples will be discussed that underscore the attractive properties and potential of this class of Au NPs as components of chemosensing assays.

## 1. Introduction

Monolayer protected gold nanoparticles (Au NPs) are stable multivalent systems (*i.e.* systems able to operate multiple molecular recognition events simultaneously) composed of a gold core of nanosized dimensions ( $d = 1 - 25$  nm) covered by a monolayer of organic molecules, typically thiols.<sup>1,2</sup> Over the past decades, Au NPs have emerged as key components of chemosensing systems.<sup>3-5</sup> This results from a combination of attractive features, amongst which is their ease of preparation, the organized structure of the monolayer and the intrinsic optoelectronic properties of the gold core. The organic monolayer is obtained through a self-assembly process driven by the formation of (most frequently) a stable Au-S bond. The result is a multivalent system with very high stability, even at very low concentrations under physiologically relevant conditions. Reproducible synthetic protocols have been developed that allow functionalization with a large variety of head groups, for use in either aqueous or organic media.<sup>6-8</sup> The optoelectronic properties of the gold core, such as surface plasmon resonance absorption, conductivity or redox behavior, can be used for signal generation as these are typically sensitive to recognition processes occurring at the monolayer surface. The synthesis and characterization of Au NPs and their application in various fields has been extensively reviewed.<sup>3-5,9</sup>

<sup>10</sup> In this Feature Article, we focus on a specific subgroup of Au NPs, namely those that contain metal binding sites in the

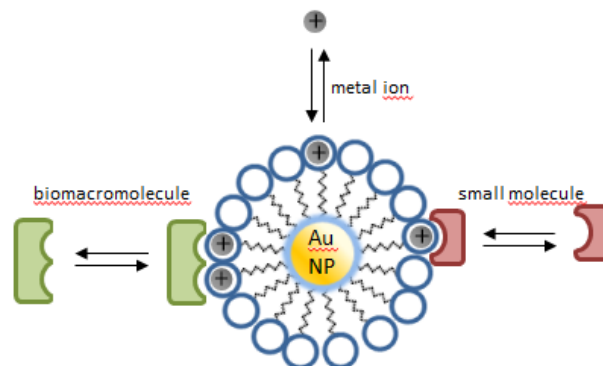


**Figure 1.** Schematic representation of a gold nanoparticle covered with a monolayer containing metal-ion binding sites and its use for the sensing of metal ions, small molecules and macromolecules.

monolayer (Figure 1). In particular, it is our intention to show that such Au NPs are particularly well-suited for chemosensing applications. We will begin by looking at the specific binding event of metal ions by the monolayer (for detection of metal ions), and demonstrate how careful design of the binding sites in the monolayer provides selectivity for specific metal ions. Alternatively, metal ions complexed in the monolayer can themselves act as recognition units for the selective interaction with small molecules or larger (bio)macromolecules. The attractiveness of these metallated monolayer protected Au NPs for sensing purposes (in addition to their application as hybrid

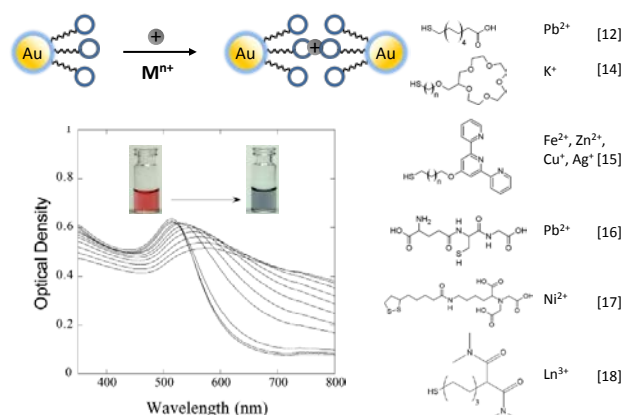


**Figure 2.** Schematic representation of the metal-ion induced aggregation of gold nanoparticles resulting in a red→blue color change.

inorganic-organic catalytic systems<sup>11</sup>) results from the possibility to create multivalent surfaces with a very high density of recognition elements able to develop strong and selective interactions with the target. In addition, the large variety of ways a detectable output signal can be generated by the system, either by changes in the properties of the gold core or by the monolayer, renders these systems perfectly suited to operate under a wide variety of conditions. It is noted that this article does not give an exhaustive overview of all contributions, but intends to illustrate the key concepts using selected examples.

## 2. Metal ion sensing

The incorporation of metal-binding sites into the monolayer of Au NPs allows for very specific interactions of these systems with metal ions. This initial metal binding event onto the monolayer of the Au NP can result in changes in the optoelectronic properties of the gold core, and numerous methods have been developed which exploit these changes to conceive novel systems suitable for sensing metal ions. Such methods have relied on changes in surface plasmon resonance absorption, conductivity or redox behavior of the Au core. Subsequently, it will be shown that by incorporating metal ions into the monolayer, highly complex, multivalent systems can be formed which can be applied to the sensing of metal ions down to the nanomolar range.

### 2.1. Colorimetric sensing

Hupp *et al.* were among the first to be challenged by the idea of exploiting the high extinction coefficients of gold nanoparticles *and* the shift of the plasmon absorption band upon nanoparticle aggregation for the detection of heavy metal ions that were otherwise 'spectroscopically silent' (Figure 2).<sup>12</sup> For this purpose, Au NPs (14 nm) were passivated with 11-mercaptoundecanoic acid, able to coordinate heavy metal ions such as Pb<sup>2+</sup>, Hg<sup>2+</sup>, and Cd<sup>2+</sup>. Indeed, the addition of either one of these metal ions, but not Zn<sup>2+</sup>, to a 2.4 nM suspension of functionalized Au particles in water containing 1.0% poly(vinyl

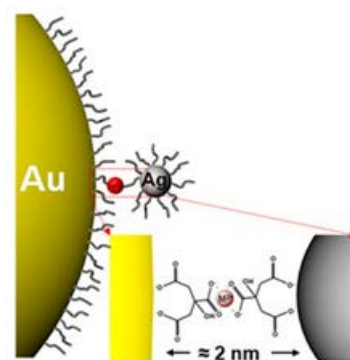


**Figure 3.** Cu<sup>2+</sup>-induced aggregation between multiple small Ag-nanoparticles and a large Au-nanoparticle. Image reproduced with permission from [20].

alcohol) (PVA) as a stabilizer resulted in a clearly visible red-to-blue color change. The reversibility of this process upon the addition of the strong chelator EDTA indicated that aggregation indeed resulted from the sandwiching of metal ions between monolayers of different nanoparticles. For this first system a rather high detection limit of around 0.4 mM for Pb<sup>2+</sup> was reported, attributed to the relatively low affinity of Pb<sup>2+</sup> for carboxylate groups and the redundancy of binding events leading to aggregation of nanoparticles. In addition to colorimetric visualization, the presence of Pb<sup>2+</sup> was also detected by hyper-Raleigh scattering (HRS), which very sensitively responded to the formation of small aggregates (as few as three). Using this technique, Pb<sup>2+</sup> concentrations down to 25 μM could be detected.

The attractive feature of this approach is the ability to tailor the metal ion selectivity simply by changing the ligand in the monolayer, provided that the metal ion is chelated by (at least) two ligands. Murphy and co-workers demonstrated the effectiveness of this approach by introducing 1,10-phenanthroline head groups, which are able to bind Li<sup>+</sup> metal ions in a 2:1 fashion.<sup>13</sup> A plot of the red-shift in the visible extinction band maximum of the gold nanoparticle against Li<sup>+</sup> concentration revealed a linear relationship, indicating that the system can be used to quantitatively detect Li<sup>+</sup> in aqueous media from 10-100 mM. Neither the addition of Na<sup>+</sup> or K<sup>+</sup> evoked a response from the system.

This approach to sensing systems has successively been exploited for the detection of a large variety of metal ions by modifying the monolayer with suitable recognition moieties such as crown ethers, terpyridines, glutathione, nitrilotriacetic acid etc. (Figure 2 and references therein).<sup>14-18</sup> Recently, Chen and Gao *et al.* reported the use of nitrotriazole-functionalized gold nanoparticles able to visually detect Hg<sup>2+</sup> in a selective manner with a detection limit down to 50 nM.<sup>19</sup> No response was observed for a large series of other metal ions up to 100 μM.

The concept of metal-ion induced aggregation has also been exploited by Yi *et al.* in more complex sensing systems.<sup>20</sup> They have reported so-called core-satellite coupled plasmonic nanoassemblies (COSA) formed by the assembly of small (2.6

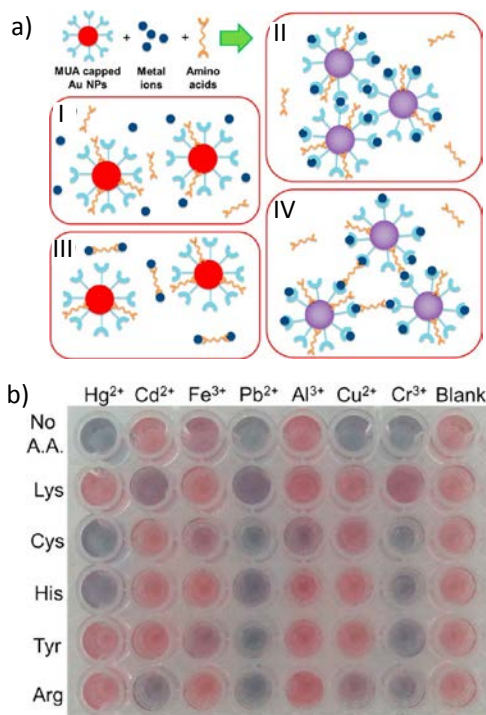


**Figure 4.** a) Schematic representation of the possible results of mixing Au NPs, metal ions, and amino acids: (I) no interaction, (II) aggregation of AuNPs induced only by the metal ion, (III) amino acids complex metal ions and prevent Au NP aggregation, and (IV) aggregation of AuNPs resulting from interaction of the metal ions with both Au NPs and amino acids. b) Colorimetric response array using 20  $\mu\text{M}$  of metal ions and a series of amino acids. Image reproduced with permission from [22].

nm) Ag<sup>+</sup> nanoparticles on the surface of much larger (50 nm) Au nanoparticles (Figure 3). This process is driven by the formation of COO<sup>-</sup>•Cu<sup>2+</sup>•OOC sandwich complexes between the citrate stabilized nanoparticles. Since the COSA assembly showed enhanced plasmon coupling (amplified intensity and spectral shift) at a single particle level, it enabled an improvement in the detection limit by at least 1000 times as compared to a single plasmonic nanoparticle. This new system was able to detect Cu<sup>2+</sup>-ions in the pM concentration range. When compared to other metal ions, Cu<sup>2+</sup> induced the strongest response owing to the higher affinity of Cu<sup>2+</sup> for the carboxylate groups. Indeed, the values observed for other divalent metals (Ni<sup>2+</sup>, Cd<sup>2+</sup>, Mg<sup>2+</sup>, Fe<sup>2+</sup>, Mn<sup>2+</sup>) were consistent with the order of binding strength between citric acid and the metal ions. In a follow-up study the system was integrated on a chip by immobilizing the gold nanoparticles on a glass substrate.<sup>21</sup> Excellent linearity of the response curves was observed at levels well below the action level of 20  $\mu\text{M}$  (or 1.3 ppm) as defined by the United States Environmental Protection Agency (EPA). In a similar theme, Weng *et al.* reported Cu<sup>2+</sup> mediated self-assembly of core satellite gold nanoparticles to develop a colorimetric sensor with a limit of detection of 2.3  $\mu\text{M}$ .<sup>21</sup>

Recently, Denizli *et al.* used Au NP aggregation and the corresponding color change to develop a colorimetric sensor

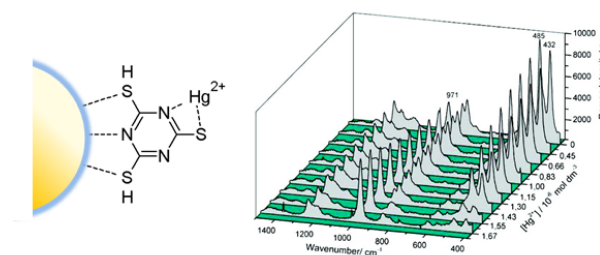


**Figure 5.** Complexation of Hg<sup>2+</sup> by TMT immobilized on Au NPs and SERS spectra as a function of the concentration of Hg<sup>2+</sup>-ions. Image reproduced with permission from [24].

array for a series of toxic metal ions (Hg<sup>2+</sup>, Cd<sup>2+</sup>, Fe<sup>3+</sup>, Pb<sup>2+</sup>, Al<sup>3+</sup>, Cu<sup>2+</sup> and Cr<sup>3+</sup>) in water.<sup>22</sup> The assay is based on the selective metal ion induced aggregation of mercaptoundecanoic acid (MUA)-capped gold nanoparticles (particle size around 30 nm) in the presence of five different amino acids (lysine, cysteine, histidine, tyrosine, and arginine) (Figure 4). The amino acids were used to complex metal ions through their amine, carboxylic acid or side-chain (such as the -SH of cysteine or -NH<sub>2</sub> group of lysine). It was shown that the selective interaction of metal ions and amino acids could either promote or diminish aggregation of Au NPs, through the various mechanisms depicted in Figure 4. For example, the presence of Pb<sup>2+</sup>, Hg<sup>2+</sup> or Cr<sup>3+</sup> causes a change in color in multiple channels (*i.e.* using different amino acids), whereas the presence of Cu<sup>2+</sup> causes aggregation only in the absence of amino acids. No change in color was observed for nine other metal ions (Ag<sup>+</sup>, Ca<sup>2+</sup>, Zn<sup>2+</sup>, Co<sup>2+</sup>, Ni<sup>2+</sup>, Sr<sup>2+</sup>, K<sup>+</sup>, Na<sup>+</sup>, Fe<sup>2+</sup>) and their mixtures. Although the sensitivity limit was quite high (20  $\mu\text{M}$ ), the straightforward protocol of the combinatorial assay should facilitate the implementation of this approach also for the sensing of other targets, such as proteins, sugars, or organic contaminants.

## 2.2. SERS

Apart from the shift induced by interparticle plasmon-plasmon coupling, the surface plasmon resonance can also cause an enhancement of the Raman scattering (SERS) of organic molecules bound to the nanoparticle surface.<sup>23</sup> This is primarily caused by an increase in the electromagnetic field at the surface of plasmonic metals and may result in an increase of the Raman signal by up to eight orders of magnitude. Particularly strong enhancements are observed in cases where the analyte is positioned in so-called 'hot-spots' between two nanoparticles. For the sensing of metal ions using SERS this implies that the systems are chemically similar to those used for the colorimetric detection discussed in the previous system. Thus, Toma *et al.* used 2,4,6-mercapto-1,3,5-triazine (TMT) attached to Au NPs as a SERS probe for the detection of heavy metal ions such as Hg<sup>2+</sup> and Cd<sup>2+</sup> (Figure 5).<sup>24</sup> A systematic decrease of the  $\nu_{\text{C-S}}$  peaks at 485 and 432 cm<sup>-1</sup> was observed upon an increase in the concentration of Hg<sup>2+</sup> ions from 200 pM



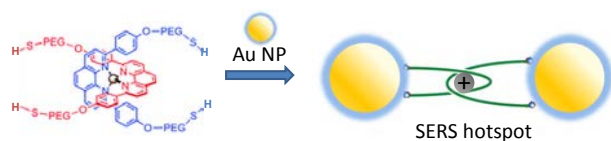


**Figure 6.** Concatenation of Au NPs by  $\text{Cu}^+$  leading to the formation of SERS hotspots.<sup>30</sup>

to 2 nM. At the same time, the intensity of the  $\beta_{\text{ring}}$  peak at  $971 \text{ cm}^{-1}$  increased suggesting the involvement of one of the triazine's nitrogen atoms in  $\text{Hg}^{2+}$  binding. Nonetheless, a practical hurdle of using SERS is control over the aggregation state of the system. Whereas the formation of small agglomerates is essential, the formation of large aggregates needs to be avoided as it complicates the quantitative and reproducible analysis of samples. Thus, Toma *et al.* added a small amount of a NaCl-solution to induce agglomeration of the NPs thus providing stable SERS signals for TMT immobilized on the Au NPs. In a more recent work, Zhao *et al.* reported a novel approach relying on bovine serum albumin (BSA) as a stabilizer to prevent nanoparticle aggregation.<sup>25</sup> In this system, *p*-aminobenzenethiol (PATP) and rhodamine 6G (R6G) were used as SERS reporters for the determination of  $\text{Ag}^+$  and  $\text{Hg}^{2+}$  ions, respectively. The systems were able to detect  $\text{Ag}^+$  and  $\text{Hg}^{2+}$  ions at low ppm and ppb concentrations, respectively, also in real water samples. The sensitivity of SERS has led to the development of various other systems for the detection of metal ions.<sup>26-29</sup>

Waterland and Telfer *et al.* have proposed a different system of intriguing molecular complexity, in which nanoparticles were 'catenated' by molecular hoops on their surfaces (Figure 6).<sup>30</sup> The mechanical interlocking of the constituent Au NPs provides a stable, yet chemically modifiable, interparticle link and positions them with a well-defined separation. The size of catenated arrays can in principle range from a dimer (with a single hoop per NP) to infinite aggregates (with multiple hoops per NP). In order to verify this, a thiol-terminated  $\text{Cu}^+$ -phenanthroline-based catenane was mixed with citrate functionalized Au NPs at various ratios. At a catenane:NP ratio of 600:1, discrete dimers and trimers were formed as evidenced by DLS and TEM. Increasing the ratio to 1500:1 led to larger aggregates until the relative amount of catenane was sufficiently high to form a passivating monolayer around the Au NPs (at a ratio of 15000:1). A fascinating feature of this system is that the catenanes are positioned at electromagnetic hotspots between the NPs which, in combination with the resonant enhancement from the MLCT transition of the catenane, gave Raman spectra with an excellent signal-to-noise ratio. Potentially, the aggregate could be an excellent sensor for  $\text{Cu}^+$ , but difficulties to demetallate the system have so far prevented this application. Another complex SERS active nanosystem was recently devised by Wang and Cui *et al.* for the low nanomolar detection and removal of  $\text{Hg}^{2+}$  and  $\text{Ag}^+$ -ions using oligonucleotide-functionalized magnetic silica sphere (MSS)@core/shell Au NPs.<sup>31</sup> Apart from their excellent SERS related properties, high

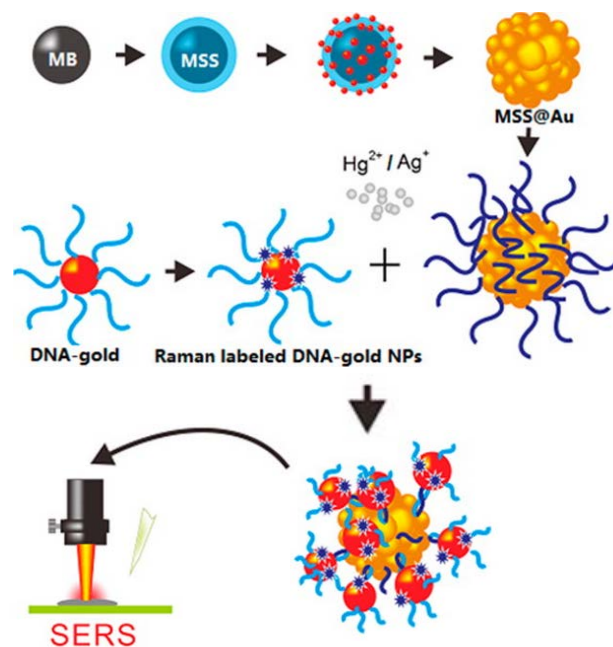


**Figure 7.** Schematic representation of the preparation of the SERS-active system MSS@Au NP for the detection of  $\text{Hg}^{2+}$  or  $\text{Ag}^+$ . Image reproduced with permission from [31].

chemical stability and biocompatibility, another advantage of these nanoparticles is that a magnet can easily remove these nanoparticles (and the complexed metal ions) from the mixture. Selectivity for  $\text{Hg}^{2+}$  and  $\text{Ag}^+$  originated from the selective interaction of these metal ions with thymine and cytosine nucleotides, respectively. In addition, 4-mercapto benzoic acid and DTNB (5,5'-dithiobis-(2-nitrobenzoic acid)) were attached to the Au NPs as Raman reporter molecules. To detect  $\text{Hg}^{2+}$ , the freshly prepared MSS@Au NPs were functionalized with T-rich DNA sequences (Figure 7). Correspondingly, other gold nanoparticles were functionalized with partially complementary sequences (leading to 5 mismatched T-T base pairs upon hybridization) to specifically recognize  $\text{Hg}^{2+}$  ions by forming ternary  $\text{T}\cdot\text{Hg}^{2+}\cdot\text{T}$  complexes. In a similar manner C-rich DNA sequences were used for  $\text{Ag}^+$  detection. The SERS signals showed excellent response for  $\text{Hg}^{2+}$  in the range of 0.1–1000 nM and for  $\text{Ag}^+$  in the range of 10–1000 nM. It was also shown that the complexed  $\text{Hg}^{2+}$  or  $\text{Ag}^+$  ions could be effectively removed from the surrounding solution by a magnet.

### 2.3. Fluorescence spectroscopy

Gold nanoclusters ranging in size from several atoms to small particles ( $< 1.2 \text{ nm}$ ) fluoresce in the blue to near-IR region.<sup>32-35</sup> Nonetheless, direct application for sensing is strongly limited by the very low quantum yields (QY) which are in the order of  $10^{-2}$ – $10^{-3}$ . However, Dickson *et al.* discovered that the quantum yield of 8 atom Au nanodots increased to around  $41 \pm 5 \%$  when encapsulated and stabilized by polyamidoamine (PAMAM) dendrimers.<sup>36</sup> This has opened the way for the development of

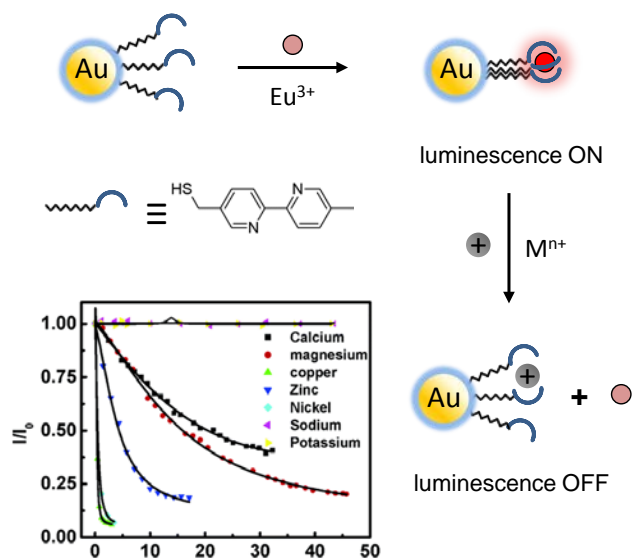


**Figure 8.** Displacement of  $\text{Eu}^{3+}$  by metal ions  $\text{M}^{n+}$  leading towards a decrease in luminescence intensity. Image reproduced with permission from [39].

sensing systems based on an alteration of the fluorescence properties of the gold core by the metal analyte. Chang *et al.* reported the use of 11-mercaptoundecanoic acid passivated Au nanoparticles for the sensing of  $\text{Hg}^{2+}$ .<sup>37</sup> Because of the relatively large size of the nanoparticles ( $2.9 \pm 0.5$  nm) a modest QY of  $3.1 \times 10^{-2}$  was observed, which was nonetheless 30000 times higher than that of non-passivated nanoparticles. Subsequently, the effect of the addition of a large number of metal ions (500 nM) on the fluorescence intensity of a 10 nM solution of Au NPs was determined. It was observed that  $\text{Hg}^{2+}$  caused the greatest decrease in fluorescence intensity, followed by  $\text{Pb}^{2+}$  and  $\text{Cd}^{2+}$ . All other studied metal ions had no effect. This phenomenon was ascribed to the ability of some metal ions to induce nanoparticle aggregation and thus quenching, which is fully in line with the data reported by Hupp *et al.* (see section 2.1).<sup>12</sup> The large fluorescence decrease observed for  $\text{Hg}^{2+}$  is caused by its relatively high affinity for simple carboxylic acids. Indeed, the selectivity could be further improved by adding 2,6-pyridinedicarboxylic acid (PDCA), which is a chelator able to compete with the nanoparticle for binding of the metal ions. The PDCA ligand forms complexes with the metal ions in solution, suppressing their interaction with the nanoparticle. In the presence of PDCA, a lower detection limit of 5.0 nM was determined for  $\text{Hg}^{2+}$  at a signal-to-noise ratio of 3. Guo *et al.* extended this concept by developing an analogous fluorescent ‘turn-off’ sensing system for  $\text{Cu}^{2+}$  based on glutathione-capped fluorescent nanoparticles.<sup>38</sup> The system demonstrated both excellent selectivity and sensitivity (LOD = 3.6 nM).

All signals generated in the sensing systems discussed so far originate from changes in the physical properties of the gold

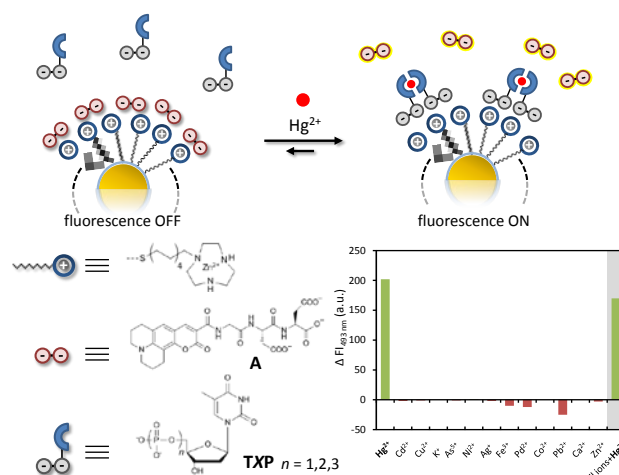


**Figure 9.** Complex formation between thymine nucleotides and  $\text{Hg}^{2+}$  leads to the formation of a ternary complex with a high affinity for the Au NP, causing displacement of the (quenched) fluorophore. Image reproduced with permission from [40a].

nuclei upon addition of the metal ion analyte. However, as pointed out in the introduction, a second reason why gold nanoparticles are so popular is the high stability of the passivating monolayers at very low concentrations in a wide variety of conditions (both aqueous and organic media). In applications focusing on the role of the monolayer, the role of the gold nucleus is often reduced to a mere support, but this is more than compensated for by the rich opportunities offered by the large variety of functional groups that can be introduced into the monolayer. To illustrate such an alternative approach to gold particle based sensing, an example by Thomas *et al.* describing a metal ion sensing system based on fluorescence is discussed.<sup>39</sup> The authors prepared gold nanoparticles ( $d \approx 4$  nm) capped with monothiol derivatives of the 2,2'-bipyridyl ligand (Figure 8). Absorption spectral studies showed that this nanosystem efficiently complexed  $\text{Eu}^{3+}$  and  $\text{Tb}^{3+}$  ions forming 1:3 complexes with the bipyridine head groups. The resulting complexes were highly phosphorescent with the Au MPC• $\text{Eu}^{3+}$  emitting in the red ( $\tau = 0.36$  ms) and the Au MPC• $\text{Tb}^{3+}$  emitting in the green ( $\tau = 0.7$  ms) regions. The strong enhancement of the line-like emissions compared to those of the free lanthanide ions originates from shielding of the encapsulated lanthanide ions by the ligands and efficient energy transfer from the bipyridine ligands to the lanthanide ions. This feature was then exploited for the detection of metal ions relying on their ability to displace lanthanide ions from the monolayer through competitive binding with the bipyridine ligands, causing a decrease in fluorescence. It was observed that the addition of alkaline earth metal ions ( $\text{Ca}^{2+}$ ,  $\text{Mg}^{2+}$ ) and transition metal ions ( $\text{Cu}^{2+}$ ,  $\text{Zn}^{2+}$ ,  $\text{Ni}^{2+}$ ) caused a strong decrease in luminescence intensity even when added at low micromolar concentrations. The addition of  $\text{Na}^+$  and  $\text{K}^+$  metal ions had no effect on the luminescence intensity.

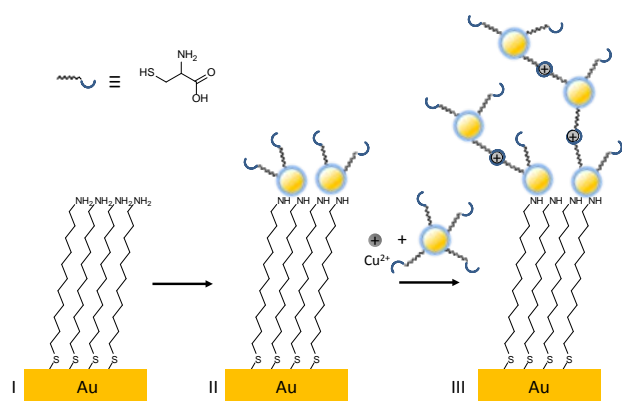


**Figure 10.** Electrochemical detection of  $\text{Cu}^{2+}$  using cysteine capped Au NPs immobilized on a gold electrode (II). The sensitivity of the system is significantly enhanced when Cys-capped Au NPs are added together with the analyte (III).<sup>41</sup>

An entirely different approach towards metal sensing was recently developed by our group based on the multivalent interactions between oligoanions and a metallated monolayer containing 1,4,7-triazacyclononane (TACN)• $\text{Zn}^{2+}$  head groups (Figure 9).<sup>40a</sup> Incorporation of metal ions into the monolayer allowed for an increase in affinity for negatively charged anions in solution, which was exploited in fluorescence-based sensing. In this system,  $\text{Hg}^{2+}$  is added to the solution of nanoparticles, a fluorescent anionic probe **A** and thymidine diphosphate (TDP). The probe and TDP compete for binding to the nanosystem and concentrations were chosen such that the major part of **A** was bound to the monolayer surface resulting in quenching of its fluorescence. The addition of  $\text{Hg}^{2+}$  resulted in the formation of a ternary complex with two TDP molecules, which has an increased affinity for the nanosystem because of a clustering of negative charges. As a result, probe **A** is displaced from the surface resulting in an increase in fluorescence. The system was able to detect  $\text{Hg}^{2+}$  with high selectivity and sensitivity (down to nM concentrations). The most interesting feature of this system lies in the way the fluorescent signal is generated. Selectivity originates from a recognition unit (here thymine) that is not connected to the nanosystem, which implies that adaptation to other targets can be performed simply by changing the recognition module without altering the nanosystem. Another feature of this system is that formation of the ternary complex between thymine and  $\text{Hg}^{2+}$  only indirectly leads to an output signal. Signal generation requires displacement of probe **A** from the Au NP through competitive binding of the ternary complex. It is the strength of this interaction that determines the efficacy at which ternary complex formation is transduced into a signal. It was indeed shown that the strength of the fluorescence output signal (for the same concentration of analyte) was dependent on the type of thymine nucleotide used (mono-, di-, or triphosphate). As such, the system bears a close resemblance to natural signal transduction pathways that rely on protein dimerization for signal generation. Recently, we have also shown the ability of this nanoparticle to select a specific nucleotide receptor (either

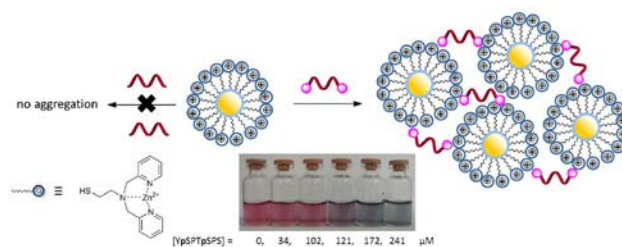


**Figure 11.** Schematic representation of NP aggregation induced by bis-phosphorylated peptides and color change as a function of the concentration of the peptide YpSPTpSPS.<sup>43</sup>

TMP or dGMP) from a library of all the nucleotides (dAMP, TMP, dGMP, dCMP) depending on the addition of target metal ions ( $\text{Hg}^{2+}$  or  $\text{Ag}^{+}$ , respectively).<sup>40b</sup>

## 2.4. Electrochemistry

Gooding *et al.* reported a very sensitive system for the electrochemical detection of  $\text{Cu}^{2+}$ .<sup>41</sup> The system relied on the use of gold electrodes covered with a monolayer of 11-amino-1-undecanethiol (Figure 10). Exposure of the electrode to citrate-stabilized gold nanoparticles resulted in their capture on the monolayer after which cysteine was added to further functionalize the gold nanoparticles as a recognition unit for  $\text{Cu}^{2+}$ . Exposure of the electrode to a solution containing  $\text{Cu}^{2+}$  resulted in an electrochemical response at around 0.1 V (against Ag/AgCl) assigned to the reduction of  $\text{Cu}^{2+}$  to  $\text{Cu}^0$ . The functionalized electrode responded to  $\text{Cu}^{2+}$  concentrations in the nano- to millimolar range. Additionally, the sensitivity of the system was dramatically improved when Cys-functionalized gold nanoparticles were added to the solution. The presence of  $\text{Cu}^{2+}$  caused aggregation of the additional nanoparticles on the electrode due to two Cys-residues interacting with a single  $\text{Cu}^{2+}$  metal ion. This feature permitted a decrease of the  $\text{Cu}^{2+}$  detection limit to as low as 1 pM, which was attributed to the fact that all the aggregated nanoparticles were electrically connected to each other via the  $\text{Cu}^{2+}$  ions.

Stellacci and Grzybowski *et al.* reported an extremely sensitive sensing system for metal ions with detection limits down to the attomolar ( $10^{-18}$  M) concentration range for toxic  $\text{CH}_3\text{Hg}^{+}$  ions.<sup>42</sup> The system is composed of two Au electrodes sputter-coated onto a glass slide and separated by a gap of around 50  $\mu\text{m}$ . The space in between the electrodes was filled with a film of gold nanoparticles functionalized with a mixture of alkane thiols and alkane thiols terminated with ethyleneglycol units. The film was then exposed to 1,14-tetradecanethiol which crosslinked the nanoparticles through thiol exchange. It was found that the conductivity of the film increased strongly upon exposure to metal ions, which facilitated charge transport between the electrodes when captured by the monolayer.

## 3. Small molecule sensing



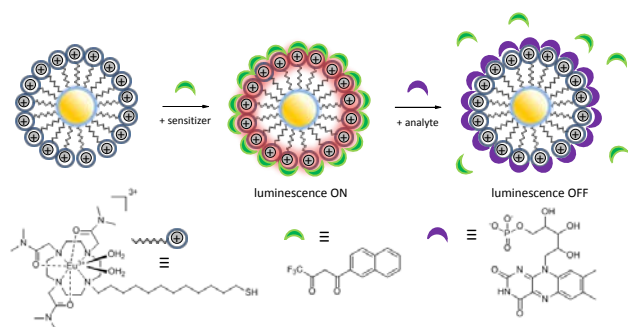


**Figure 12.** Binding of a diketone sensitizer to  $\text{Eu}^{3+}$ -containing monolayer causes a strong enhancement of the luminescence. Displacement of the antenna by an analyte results in a decrease in luminescence.<sup>44</sup>

The sensing of small molecules poses the challenge of developing receptors that can efficiently discriminate between analytes that may be structurally very similar. It will be shown in this section that metallated monolayer protected NPs are very attractive for that purpose, because metal ions in the monolayer can enhance the binding affinity of small molecules for the monolayer surface. In addition, metal ions can induce selectivity because of preferential binding to certain functional groups present in the analyte.

This potential is well exemplified by an example from Yuan *et al.*, which exploited the change in color upon nanoparticle aggregation for the detection of bis-phosphorylated peptides (Figure 11).<sup>43</sup> These are important targets as protein phosphorylation plays an important role in intracellular signaling and the presence of abnormally phosphorylated peptides in blood serum may signify the presence of a pathology. The sensing system was composed of dipicolylamine• $\text{Zn}^{2+}$  complexes appended to gold nanoparticles by means of a small spacer. A red-to-blue color change in the gold nanoparticle solution was observed when bis-phosphorylated peptides were added at high  $\mu\text{M}$  concentrations. TEM images confirmed the aggregated state of the nanoparticles. Importantly, non-phosphorylated peptides or mono-phosphorylated peptides failed to induce aggregation, suggesting that the interaction of the two phosphate groups in the bis-phosphorylated peptide with two different nanoparticles is the driving force for aggregation.

Gunnlaugsson *et al.* reported a very elegant system for the detection of biologically relevant molecules.<sup>44</sup> The key component of the sensor were gold nanoparticles passivated with alkyl thiols containing a heptadentate macrocyclic ligand for complexation of  $\text{Eu}^{3+}$  (Figure 12). Lanthanides possess many highly desirable photo-physical properties that are ideal for biological applications. These include narrow line-like emission bands and most notably, long-lived excited states, which enables the use of time-resolved detection. The resulting cyclen:Eu(III) functionalized Au MPCs were fully water soluble, but their luminescence was quenched through vibrational deactivation by coordinating water molecules. Nonetheless, the displacement of bound water molecules by a  $\beta$ -diketone antenna led to a strongly luminescent system upon

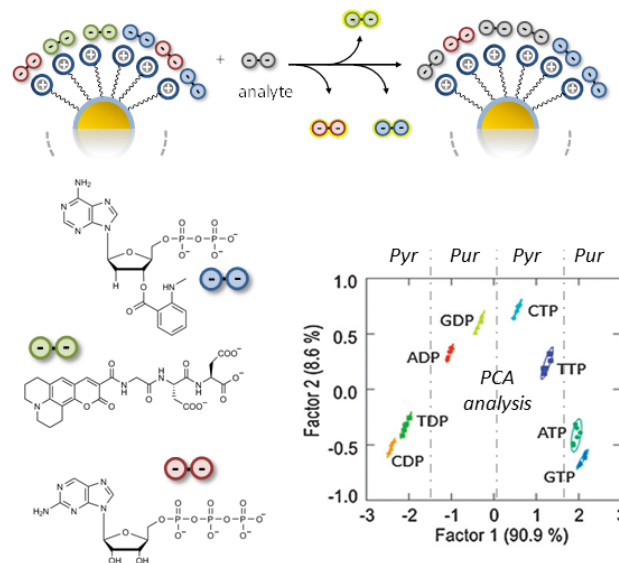


**Figure 13.** Multi-indicator displacement assay used for the discrimination of all di- and trinucleotides XDP and XTP. The monolayer is identical to the one depicted in Figure 8. Image reproduced with permission from [47].

excitation of the antenna at 336 nm. It was found that addition of phosphate- and carboxylate-containing molecules (such as ATP, ADP, NADP or coumaric and pantothenic acid) led to displacement of the antennae and consequently, a decrease in luminescence. Remarkably, flavin mononucleotide was the only anion able to displace completely the antenna molecule after adding 450 equivalents with respect to the head group, leading to complete luminescence quenching.

Rastrelli, Mancin *et al.* demonstrated that the paramagnetic relaxation enhancement caused by  $\text{Gd}^{3+}$  lanthanide ions complexed in the monolayer resulted in a cancellation of the nearby spins in the NMR spectrum.<sup>45</sup> This provided a powerful tool to study the surface morphology of a mixed monolayer composed of two different thiols. Also, it was shown that pseudocontact NMR shifts induced by  $\text{Yb}^{3+}$  and  $\text{Tb}^{3+}$  ions complexed in the monolayer allowed mapping of the position of small organic molecules (such as methyl benzoate and potassium *p*-toluenesulfonate) bound to the monolayer.<sup>46</sup>

In collaboration with the Severin-group, we recently showed that the Gunnlaugsson-approach, which is essentially a displacement assay, can be extended to the pattern-based sensing of nucleotides using TACN• $\text{Zn}^{2+}$  functionalized Au NPs.<sup>47</sup> In this system, the high affinity of the metallated monolayer protected Au NPs for oligoanions is exploited to assemble three different anionic fluorescent indicators on the monolayer surface (Figure 13). When bound to the monolayer, the fluorescence of these probes is quenched by the gold nucleus. The addition of di- and trinucleotides (as analytes) to this system results in a displacement of the probes and a turn-on of their fluorescence. Since the affinity of the oligoanion for the Au NPs is governed by a combination of electrostatic and



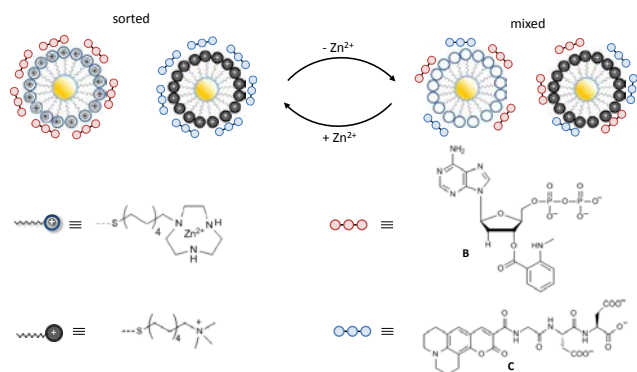


**Figure 14.** Self-sorting and mixing of phosphates and carboxylates on the surface of two different monolayers regulated by  $Zn^{2+}$ . Image reproduced with permission from [49].

hydrophobic interactions, a distinct response is observed for each nucleotide. Repetition of the displacement assay with  $Cu^{2+}$  instead of  $Zn^{2+}$  and combination of the two data sets allowed for quantitative discrimination of all nucleotides in the low  $\mu M$  concentration region.

Two follow-up studies with the same system illustrated the important role of metal ions in the monolayer as regulatory elements for controlling the selectivity and affinity between small molecules and the nanosystem. The first study revealed that  $Zn^{2+}$  metal ions play a crucial role in the assembly process by increasing the charge density of the monolayer.<sup>48</sup> As a consequence, this permits an increased number of anionic probes (such as ATP) to bind concurrently to the monolayer surface. Indeed, the removal of  $Zn^{2+}$  metal ions from the monolayer upon the addition of  $N,N,N',N'$ -tetrakis(2-pyridylmethyl)ethylenediamine (TPEN), which is a strong chelator for  $Zn^{2+}$ , resulted in the release of an ATP analogue from the surface. Adding a new batch of  $Zn^{2+}$  metal ions to the system to reform the  $TACN \cdot Zn^{2+}$  complexes reversed this process. This implies that the  $Zn^{2+}$  ions act as regulatory elements to the valency of the nanosystem by determining the number of small molecules bound to the surface. Such 'post-synthetic' control over the valency offers a new perspective for the active regulation of binding strength between a dynamic system and a multivalent biotarget.

A second study revealed that the presence of  $Zn^{2+}$ -metal ions in the monolayer rendered the system selective for phosphates over carboxylates (Figure 14).<sup>49</sup> This was shown by competition experiments between fluorescent ADP-derivative **B** and the fluorescent peptide **C** having the same number of charges. Indeed, only minor selectivity was observed in the absence of  $Zn^{2+}$ . Also, no preferential binding was observed when a different Au NP with quaternary ammonium head groups was used (Figure 14). This led to the interesting observation that, in the presence of  $Zn^{2+}$ , the addition of both nanosystems to a mixture of carboxylate and phosphate probes resulted in self-sorting of the two probes with each of them residing on a different nanoparticle surface. The

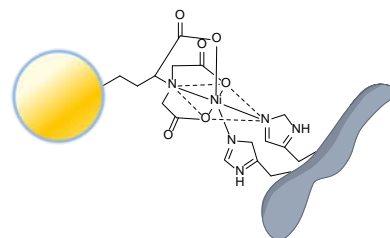


**Figure 15.** Schematic representation of complex formation between a  $Ni^{2+}$ -NTA functionalized Au NPs and a His-tagged protein.

removal/addition of  $Zn^{2+}$  metal ions from the system can be used to revert the system from an ordered to a disordered state and vice versa. The possibility to control the location and transport of populations of molecules in a complex mixture creates a new perspective for the development of innovative complex catalytic systems that mimic Nature.

## 4. Biomacromolecule sensing

A large part of gold nanoparticle research is dedicated to their interaction with large biomolecules such as DNA and proteins.<sup>3, 5</sup> In part, this originates from the intrinsic importance of these analytes, but it is also caused by the fact that functionalized nanoparticles are particularly suited for this purpose. Their multivalent nature permits multiple interactions between the sensing system and the target, which favorably affects both affinity and selectivity, just like in Nature. For this class of targets, metallated monolayer protected Au NPs are very useful because of the attractive features mentioned in the previous section, *i.e.* high affinity and selectivity originating from interactions with the metal ions, are typically amplified when interacting with a multivalent (bio)target.

### 4.1. DNA sensing

$Ru^{2+}$ -polypyridyl complexes have been applied extensively as sensitive and structure-specific DNA probes because of their excellent photophysical properties. Gunnlaugsson, Williams *et al.* functionalized gold nanoparticles with these complexes to obtain highly sensitive, biocompatible systems for imaging.<sup>50,51</sup> The high local concentration of fluorescence moieties strongly enhances the signal-to-noise ratio, which makes the system attractive for imaging. UV-vis titrations showed that the water-soluble systems had a strong affinity for salmon testes DNA with binding constants in the order of  $10^5 M^{-1}$ . Further confirmation for DNA binding was obtained from ethidium bromide displacement assays and confocal microscopy measurements. The systems were then tested for their cellular uptake properties by incubating HeLa cells. Fluorescence confocal laser scanning microscopy confirmed the efficient

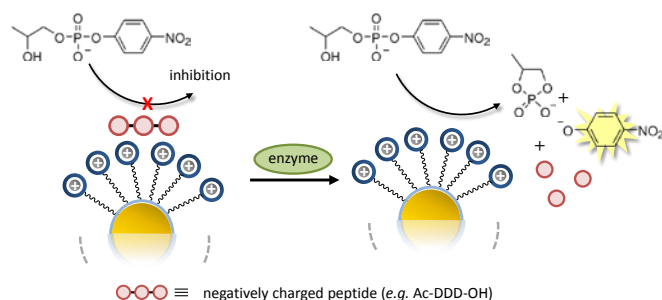


**Figure 16.** Schematic representation of an enzyme assay relying on catalytic signal amplification.<sup>56</sup> Fragmentation of a negatively charged peptide substrate, which also act as inhibitor of catalytic activity of Au NPs, by the target enzyme results in an activation of Au NPs (for the structure of Au NPs see Figure 14).

uptake and internal localization of the complexes in the cytoplasm and nucleus. The nuclear localization of the systems was confirmed by co-staining with DAPI. An important observation was that the nanosystems did not show significant induction of apoptosis.

#### 4.2. Protein sensing

The strong affinity of  $\text{Ni}^{2+}$ -nitrilotriacetic acid (NTA) complexes for His-rich sequences is widely applied for protein purification (Figure 15). It is well known that the affinity increases strongly in cases where multiple  $\text{Ni}^{2+}$ -NTA complexes act simultaneously with the target. This makes it very attractive to create multivalent systems in which multiple  $\text{Ni}^{2+}$ -NTA complexes are positioned in close vicinity. Already, back in 1999, Hainfeld *et al.* coined the term ‘PeptideGold’, referring to gold nanoparticles passivated with NTA-dipeptide-thiols.<sup>52</sup> By using a combination of chromatography, blotting and scanning transmission electron microscopy, it was demonstrated that these nanoparticles targeted a 6-His-motif attached to an adenovirus ‘knob’ protein. The high affinity of the multivalent nanoconstruct for the His-tag became evident from competition experiments with imidazole. Whereas a 0.1 N solution of imidazole was sufficient to strip the Ad12 knob protein from a Ni-column, it did not fully disrupt binding of the nanoparticle-protein complex. In a recent study by Wright *et al.* this binding interaction was used to induce aggregation of the nanoparticles in multivalent biosystems detectable by spectrophotometric changes.<sup>53</sup> Li *et al.* developed bifunctional Au- $\text{Fe}_3\text{O}_4$  nanoparticles with  $\text{Ni}^{2+}$ -coordinated N-[ $\text{N}_\alpha, \text{N}_\alpha$ -bis(carboxymethyl)-L-lysine]-16-mercaptohexadecanamide immobilized on the Au shell. This material was suitable for the purification of any 6-His tagged protein by chelation followed by magnetic separation.<sup>54</sup>

Following the successful application of luminescent  $\text{Eu}^{3+}$ -gold nanoparticle systems for the detection of phosphate anions, Gunnlaugsson and Comby studied the interaction of the same system with bovine serum albumin (BSA), which is the main plasma carrier for a wealth of both endogenous and exogenous

substances.<sup>55</sup> These studies were motivated by the fact that previous studies had shown that BSA was able to complex molecular lanthanide-complexes. Binding interactions of the system with BSA were studied using UV-vis spectroscopy as well as steady state and time-resolved fluorescence spectroscopy. These studies revealed that the luminescence emission of  $\text{Eu}(\text{III})$  was almost completely quenched upon the addition of BSA. However, in contrast to the interaction with phosphate anions (see section 3) this was not caused by displacement of the antenna, but rather the result of direct interaction between the antenna and the protein. This system was then employed as a luminescent reporter for the binding of drugs to BSA. In this setup, the drug competes with  $\text{Ni}^{2+}$ -nitrilotriacetic acid (NTA) for binding to BSA and its displacement would restore the  $\text{Eu}$ -luminescence. Competitive titrations using ibuprofen and warfarin showed that NTA was located in the binding site II of BSA and that the presence of warfarin, a site I drug, did not interfere with the detection of site II ibuprofen.

We have reported a gold nanoparticle based sensing system for the detection of proteolytic enzymes (Figure 16).<sup>56</sup> The enzyme assay relies on the use of a peptidic enzyme substrate that also functions as an inhibitor of  $\text{TACN}\cdot\text{Zn}^{2+}$  catalytic activity, which are functionalized onto gold nanoparticles. Upon hydrolysis by the enzyme, the peptidic substrate/inhibitor is fragmented, losing affinity for the monolayer surface. As a consequence, catalytic activity of the  $\text{TACN}\cdot\text{Zn}^{2+}$ -functionalised monolayer is restored, resulting in production of the *p*-nitrophenolate anion as a reporter molecule. The selectivity of the system for different enzymes could be tuned simply by changing the peptide sequence employed as substrate/inhibitor. An attractive feature of this system is the use of catalytic signal amplification, which generates a signal subject to the turn-over number of the catalyst. This permits much higher sensitivity compared to classical assays relying on the production of a single reporter for each substrate molecule cleaved. In this particular system, the  $\text{Zn}^{2+}$  metal ions present in the monolayer play a dual role, both by enhancing the affinity for the peptidic substrate/inhibitor and by creating catalytic pockets composed of two  $\text{TACN}\cdot\text{Zn}^{2+}$ -complexes.<sup>57</sup>

#### 4.3. Cellular uptake

Pikramenou *et al.* reported on the cellular uptake of luminescent lanthanide-coated nanoparticles. In this study, gold nanoparticles were functionalized with a red luminescent  $\text{Eu}^{3+}$ -probe (bound to a diethylenetriaminepentaacetic acid (DTPA)-bisamide ligand with a quinoline sensitizer and thiols for surface anchoring) and multiple copies of the pH low insertion peptide (pHLIP) sequence.<sup>58</sup> This peptide mediates translocation across membranes by spontaneously forming a helical structure upon a decrease in pH to 6.5, which in vivo may be caused by certain pathologies. It was shown that this transition could be used to control the delivery of the nanoprobes into platelets in just a few minutes. At pH 7.4, no membrane translocation was detected. Luminescence lifetime

measurements confirmed that  $\text{Eu}^{3+}$  remained attached to the nanoparticles also inside the cells.

## 5. Conclusions and perspective

The examples discussed in the previous section illustrate the opportunities of incorporating metal-binding sites into the monolayer of gold nanoparticles. The careful design of these coordination sites permits the selective binding of metal ions. This in turn enables the creation of highly sensitive sensing systems when metal-ion complexation is able to alter one of the many properties of the gold nanoparticles itself. On the other hand, the presence of stable (non-saturated) metal complexes in the monolayer can also be used to create selective binding sites for small molecules. In these systems the metal ion becomes an element that introduces selectivity, while also enhancing affinity due to the relatively high strength of coordination bonds when compared to other noncovalent interactions (such as electrostatic interactions and hydrogen bonding). The affinity is further enhanced when multiple metal ions are simultaneously involved in the binding of the analyte. Evidently, this possibility is a direct advantage of the multivalent nature of monolayer protected gold nanoparticles. The ease of preparation and straightforward access to variants is another distinct advantage of these systems. Although the systems employed so far have been of relatively low complexity, one can imagine the incorporation of additional ligands on existing nanoparticles in order to create heterogeneous systems of significantly higher complexity. Such heterometallic systems could find application as highly selective sensing systems, or one could also envision their use as multivalent platforms for the concentration, organization and reaction of small molecules.

## 6. Acknowledgments

Financial support from the ERC (StG-239898), the University of Padova (International Mobility Program and CPDA138148) and COST (CM1304) is acknowledged.

## Notes and references

<sup>a</sup>Department of Chemical Sciences, University of Padova, Via Marzolo 1, 35131 Padova, Italy. leonard.prins@unipd.it

1. A. C. Templeton, M. P. Wuelving and R. W. Murray, *Acc. Chem. Res.*, 2000, **33**, 27-36.
2. M. C. Daniel and D. Astruc, *Chem. Rev.*, 2004, **104**, 293-346.
3. D. A. Giljohann, D. S. Seferos, W. L. Daniel, M. D. Massich, P. C. Patel and C. A. Mirkin, *Angew. Chem. Int. Ed.*, 2010, **49**, 3280-3294.
4. U. H. F. Bunz and V. M. Rotello, *Angew. Chem. Int. Ed.*, 2010, **49**, 3268-3279.
5. K. Saha, S. S. Agasti, C. Kim, X. N. Li and V. M. Rotello, *Chem. Rev.*, 2012, **112**, 2739-2779.
6. P. X. Zhao, N. Li and D. Astruc, *Coord. Chem. Rev.*, 2013, **257**, 638-665.
7. M. Brust, M. Walker, D. Bethell, D. J. Schiffrin and R. Whyman, *Chem. Commun.*, 1994, 801-802.
8. N. R. Jana and X. G. Peng, *J. Am. Chem. Soc.*, 2003, **125**, 14280-14281.
9. A. J. Mieszawska, W. J. M. Mulder, Z. A. Fayad and D. P. Cormode, *Mol. Pharm.*, 2013, **10**, 831-847.
10. H. Wei and E. K. Wang, *Chem. Soc. Rev.*, 2013, **42**, 6060-6093.
11. G. Pieters and L. J. Prins, *New. J. Chem.*, 2012, **36**, 1931-1939.
12. Y. J. Kim, R. C. Johnson and J. T. Hupp, *Nano Lett.*, 2001, **1**, 165-167.
13. S. O. Obare, R. E. Hollowell and C. J. Murphy, *Langmuir*, 2002, **18**, 10407-10410.
14. L. E. Russell, R. R. Pompano, K. W. Kittredge and M. C. Leopold, *J. Mater. Sci.*, 2007, **42**, 7100-7108.
15. T. B. Norsten, B. L. Frankamp and V. M. Rotello, *Nano Lett.*, 2002, **2**, 1345-1348.
16. F. Chai, C. Wang, T. Wang, L. Li and Z. Su, *ACS Appl. Mater. Interfaces*, 2010, **2**, 1466-1470.
17. Z. Krpetic, L. Guerrini, I. A. Larmour, J. Reglinski, K. Faulds and D. Graham, *Small*, 2012, **8**, 707-714.
18. C. E. Lisowski and J. E. Hutchison, *Anal. Chem.*, 2009, **81**, 10246-10253.
19. X. J. Chen, Y. B. Zu, H. Xie, A. M. Kemas and Z. Q. Gao, *Analyst*, 2011, **136**, 1690-1696.
20. I. Choi, H. D. Song, S. Lee, Y. I. Yang, T. Kang and J. Yi, *J. Am. Chem. Soc.*, 2012, **134**, 12083-12090.
21. a) H. D. Song, I. Choi, S. Lee, Y. I. Yang, T. Kang and J. Yi, *Anal. Chem.*, 2013, **85**, 7980-7986. b) Z. Weng, H. Wang, J. Vongsvivut, R. Li, A. M. Glushenkov, J. He, Y. Chen, C. J. Barrow and W. Yang, *Anal. Chim. Acta*, 2013, **803**, 128-134.
22. G. Sener, L. Uzun and A. Denizli, *ACS Appl. Mater. Interfaces*, 2014, **6**, 18395-18400.
23. X. M. Qian and S. M. Nie, *Chem. Soc. Rev.*, 2008, **37**, 912-920.
24. V. M. Zamarion, R. A. Timm, K. Araki and H. E. Toma, *Inorg. Chem.*, 2008, **47**, 2934-2936.
25. W. Ji, L. Chen, X. Xue, Z. Guo, Z. Yu, B. Zhao and Y. Ozaki, *Chem. Commun.*, 2013, **49**, 7334-7336.
26. R. A. Alvarez-Puebla, D. S. dos Santos, Jr. and R. F. Aroca, *Analyst*, 2007, **132**, 1210-1214.
27. F. Chai, C. Wang, T. Wang, Z. Ma and Z. Su, *Nanotechnology*, 2010, **21**, 025501.
28. T. Senapati, D. Senapati, A. K. Singh, Z. Fan, R. Kanchanapally and P. C. Ray, *Chem. Commun.*, 2011, **47**, 10326-10328.
29. J. Yin, T. Wu, J. Song, Q. Zhang, S. Liu, R. Xu and H. Duan, *Chem. Mater.*, 2011, **23**, 4756-4764.
30. C. A. Otter, P. J. Patty, M. A. K. Williams, M. R. Waterland and S. G. Telfer, *Nanoscale*, 2011, **3**, 941-944.
31. M. Liu, Z. Wang, S. Zong, H. Chen, D. Zhu, L. Wu, G. Hu and Y. Cui, *ACS Appl. Mater. Interfaces*, 2014, **6**, 7371-7379.
32. J. P. Wilcoxon, J. E. Martin, F. Parsapour, B. Wiedenman and D. F. Kelley, *J. Chem. Phys.*, 1998, **108**, 9137-9143.
33. S. Link, A. Beeby, S. FitzGerald, M. A. El-Sayed, T. G. Schaaff and R. L. Whetten, *J. Phys. Chem. B*, 2002, **106**, 3410-3415.

34. J. Zheng, C. W. Zhang and R. M. Dickson, *Phys. Rev. Lett.*, 2004, **93**, 077402.
35. G. Wang, R. Guo, G. Kalyuzhny, J.-P. Choi and R. W. Murray, *J. Phys. Chem. B*, 2006, **110**, 20282-20289.
36. J. Zheng, J. T. Petty and R. M. Dickson, *J. Am. Chem. Soc.*, 2003, **125**, 7780-7781.
37. C.-C. Huang, Z. Yang, K.-H. Lee and H.-T. Chang, *Angew. Chem. Int. Ed.*, 2007, **46**, 6824-6828.
38. W. Chen, X. Tu and X. Guo, *Chem. Commun.*, 2009, 1736-1738.
39. B. I. Ipe, K. Yoosaf, K. G. Thomas, *J. Am. Chem. Soc.* 2006, **128**, 1907-1913.
40. a) S. Maiti, C. Pezzato, S. G. Martin and L. J. Prins, *J. Am. Chem. Soc.*, 2014, **136**, 11288-11291. b) S. Maiti and L. J. Prins, *Chem. Commun.*, 2015, **51**, 5714-5716.
41. J. J. Gooding, J. Shein and L. M. H. Lai, *Electrochem. Commun.*, 2009, **11**, 2015-2018.
42. E. S. Cho, J. Kim, B. Tejerina, T. M. Hermans, H. Jiang, H. Nakanishi, M. Yu, A. Z. Patashinski, S. C. Glotzer, F. Stellacci and B. A. Grzybowski, *Nat. Mater.*, 2012, **11**, 978-985.
43. S. Zhang, J. Wang, L. Han, C. Li, W. Wang and Z. Yuan, *Sens. Actu. B - Chem.*, 2010, **147**, 687-690.
44. J. Massue, S. J. Quinn and T. Gunnlaugsson, *J. Am. Chem. Soc.*, 2008, **130**, 6900-6901.
45. G. Guarino, F. Rastrelli, P. Scrimin and F. Mancin, *J. Am. Chem. Soc.*, 2012, **134**, 7200-7203.
46. G. Guarino, F. Rastrelli and F. Mancin, *Chem. Commun.*, 2012, **48**, 1523-1525.
47. C. Pezzato, B. Lee, K. Severin and L. J. Prins, *Chem. Commun.*, 2013, **49**, 469-471.
48. G. Pieters, C. Pezzato and L. J. Prins, *J. Am. Chem. Soc.*, 2012, **134**, 15289-15292.
49. C. Pezzato, P. Scrimin and L. J. Prins, *Angew. Chem. Int. Ed.*, 2014, **53**, 2104-2109.
50. R. B. P. Elmes, K. N. Orange, S. M. Cloonan, D. C. Williams and T. Gunnlaugsson, *J. Am. Chem. Soc.*, 2011, **133**, 15862-15865.
51. S. J. Bradberry, A. J. Savyasachi, M. Martinez-Calvo and T. Gunnlaugsson, *Coord. Chem. Rev.*, 2014, **273**, 226-241.
52. J. F. Hainfeld, W. Q. Liu, C. M. R. Halsey, P. Freimuth and R. D. Powell, *J. Struct. Biol.*, 1999, **127**, 185-198.
53. J. D. Swartz, C. P. Gulka, F. R. Haselton and D. W. Wright, *Langmuir*, 2011, **27**, 15330-15339.
54. J. Bao, W. Chen, T. Liu, Y. Zhu, P. Jin, L. Wang, J. Liu, Y. Wei and Y. Li, *ACS Nano*, 2007, **1**, 293-298.
55. S. Comby and T. Gunnlaugsson, *ACS Nano*, 2011, **5**, 7184-7197.
56. R. Bonomi, A. Cazzolaro, A. Sansone, P. Scrimin and L. J. Prins, *Angew. Chem. Int. Ed.*, 2011, **50**, 2307-2312.
57. G. Zaupa, C. Mora, R. Bonomi, L. J. Prins and P. Scrimin, *Chem. Eur. J.*, 2011, **17**, 4879-4889.
58. A. Davies, D. J. Lewis, S. P. Watson, S. G. Thomas and Z. Pikramenou, *Proc. Natl. Acad. Sci. USA*, 2012, **109**, 1862-1867.